INTERNATIONAL JOURNAL FOR NUMERICAL METHODS IN FLUIDS
Int. J. Numer. Meth. Fluids 2009; **60**:1149–1172
Published online 23 October 2008 in Wiley InterScience (www.interscience.wiley.com). DOI: 10.1002/fld.1931

A fast method for solving fluid–structure interaction problems numerically

C. M. Murea*, † and S. Sy‡

Laboratoire de Mathématiques, Informatique et Applications, Université de Haute-Alsace, 4, rue des Frères Lumière, 68093 Mulhouse Cedex, France

SUMMARY

The paper presents a semi-implicit algorithm for solving an unsteady fluid–structure interaction problem. The algorithm for solving numerically the fluid–structure interaction problems was obtained by combining the backward Euler scheme with a semi-implicit treatment of the convection term for the Navier–Stokes equations and an implicit centered scheme for the structure equations. The structure is governed either by the linear elasticity or by the non-linear St Venant–Kirchhoff elasticity models. At each time step, the position of the interface is predicted in an explicit way. Then, an optimization problem must be solved, such that the continuity of the velocity as well as the continuity of the stress hold at the interface. During the Broyden, Fletcher, Goldforb, Shano (BFGS) iterations for solving the optimization problem, the fluid mesh does not move, which reduces the computational effort. The term 'semi-implicit' used for the fully algorithm means that the interface position is computed explicitly, while the displacement of the structure, velocity and the pressure of the fluid are computed implicitly. Numerical results are presented. Copyright © 2008 John Wiley & Sons, Ltd.

Received 25 June 2007; Revised 26 May 2008; Accepted 21 August 2008

KEY WORDS: fluid–structure interaction problems; arbitrary Lagrangian Eulerian; flow in moving domain

1. INTRODUCTION

We consider an unsteady incompressible flow through a channel with elastic wall. This kind of fluid–structure interaction problem is of considerable interest in bio-mechanics.

A family of explicit algorithms known also as staggered was successfully employed for the aeroelastic applications [1]. The numerical results presented in [2] show that an explicit algorithm based on the leap-frog scheme for the structure and on the backward Euler scheme for the fluid is unstable for simulation of blood flow in large arteries. The instability does not depend on the

*Correspondence to: C. M. Murea, Laboratoire de Mathématiques, Informatique et Applications, Université de Haute-Alsace, 4, rue des Frères Lumière, 68093 Mulhouse Cedex, France.
†E-mail: Cornel.Murea@uha.fr, http://www.edp.lmia.uha.fr/murea/
‡E-mail: soyibou.sy@uha.fr

time step but on the mass densities of fluid and structure and on the geometry. The theoretical result presented in [3] confirms that. In [4], explicit algorithms based on the generalized α method for the structure and three backward differencing schemes for the fluid will get unstable when the mass density ratio of fluid and structure is greater than a certain threshold.

Implicit algorithms have been developed based on fixed point strategies [2, 5, 6]. Using the transpiration technique [7, 8], the convergence can be accelerated. Faster algorithms are obtained when the derivative is employed. A block Newton algorithm was used in [9], where the derivative of the operators are approached by finite differences. The Newton method was employed in [10], where the derivative of the operator was replaced by a simpler operator and in [11] where the gradient was computed analytically. The Newton method that incorporate the linearization of the fully discretized model was described in [12]. Space–time finite element techniques for fluid–structure interaction problems are presented in [13].

Other implicit algorithms based on optimal control model was investigated in [14, 15] in the steady case. We can use the same strategy for the unsteady fluid–structure interaction problems and at each time step, we have to solve an optimization problem. The gradient of the cost function is approached by finite differences in [16] where it is proved the superiority of the Broyden, Fletcher, Goldforb, Shano (BFGS) method in comparison with the modified Newton method (Newton with line search), when moderate time step is used. The analytic formula of the gradient of the cost function is presented in [17].

Since the implicit algorithms are very expensive in computational time, a semi-implicit strategy based on the Chorin–Temam projection scheme for incompressible flows is introduced in [18]. The term semi-implicit means that the interface position is computed explicitly, while the displacement of the structure, velocity and the pressure of the fluid are computed implicitly. A related semi-implicit algorithm is presented in [19], where the structure equation is embedded into the fluid equations.

The aim of this paper is to present a semi-implicit algorithm based on the optimal control idea. The numerical results prove that the computational effort is reduced in comparison with the implicit algorithm, while the computed solutions obtained by the two methods are almost the same.

2. STATEMENT OF THE PROBLEM

Let us denote by Ω^{S} the undeformed structure domain. We shall assume that its boundary admits the decomposition $\partial\Omega^{\mathrm{S}}=\Gamma_{\mathrm{D}}\cup\Gamma_{\mathrm{N}}\cup\Gamma_0$. On Γ_{D} the displacement will be prescribed and on Γ_{N} the stress is known.

The initial fluid domain Ω_0^{F} is bounded by: Σ_1 the inlet section, Σ_2 the bottom boundary, Σ_3 the outlet section and Γ_0 the top boundary (see Figure 1, at the left). The boundary Γ_0 is common of both domains and it represents the initial position of the fluid–structure interface.

Under the action of the fluid stress, the structure will be deformed. At the time instant t, the fluid occupies the domain Ω_t^{F} bounded by the moving interface Γ_t and by the rigid boundary $\Sigma=\Sigma_1\cup\Sigma_2\cup\Sigma_3$ (see Figure 1, at the right).

We have assumed that the fluid is governed by the Navier–Stokes equations, while either linear elasticity or non-linear St Venant–Kirchhoff elasticity models have been employed for the structure. At each time instant $t\in[0,T]$, we are interested to know: the structure displacement $\mathbf{u}=(u_1,u_2)^{\mathrm{T}}$: $\Omega^{\mathrm{S}}\times[0,T]\to\mathbb{R}^2$, the fluid domain Ω_t^{F}, the fluid velocity $\mathbf{v}(t)=(v_1(t),v_2(t))^{\mathrm{T}}:\Omega_t^{\mathrm{F}}\to\mathbb{R}^2$ and the fluid pressure $p(t):\Omega_t^{\mathrm{F}}\to\mathbb{R}$.

DOI: 10.1002/fld

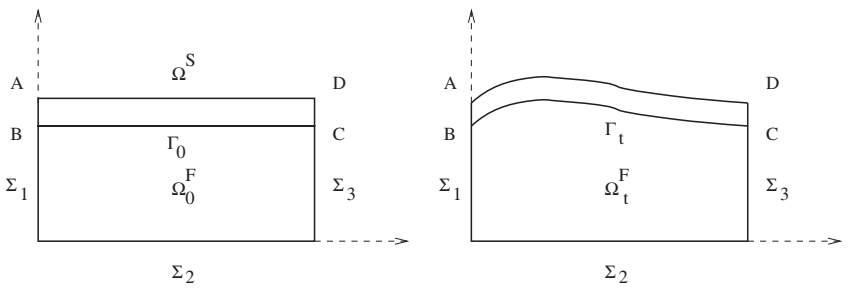

Figure 1. Initial (left) and intermediate (right) geometrical configuration.

Linear elasticity equations:

$$\rho^S \frac{\partial^2 \mathbf{u}}{\partial t^2} - \nabla \cdot \sigma^S = \mathbf{f}^S \quad \text{in } \Omega^S \times (0,T) \tag{1}$$

$$\sigma^S = \lambda^S (\nabla \cdot \mathbf{u}) \mathbb{I} + 2\mu^S \varepsilon(\mathbf{u}) \tag{2}$$

$$\varepsilon(\mathbf{u}) = \tfrac{1}{2}(\nabla \mathbf{u} + (\nabla \mathbf{u})^T) \tag{3}$$

$$\mathbf{u} = 0 \quad \text{on } \Gamma_D \times (0,T) \tag{4}$$

$$\sigma^S \mathbf{n}^S = 0 \quad \text{on } \Gamma_N \times (0,T) \tag{5}$$

where $\rho^S > 0$ is the mass density of the structure, $\lambda^S > 0$ and $\mu^S > 0$ are the Lamé parameters, $\mathbf{f}^S : \Omega^S \times (0,T) \to \mathbb{R}^2$ is the applied volume force per unit area, $\varepsilon(\mathbf{u})$ is the linearized strain tensor, $\mathbb{I}$ is the identity matrix, $\mathbf{n}^S$ is the unit outer normal vector along the boundary $\partial\Omega^S$.

Navier–Stokes equations:

$$\rho^F \left(\frac{\partial \mathbf{v}}{\partial t} + (\mathbf{v} \cdot \nabla)\mathbf{v} \right) - \nabla \cdot \sigma^F = \mathbf{f}^F \quad \forall t \in (0,T) \ \ \forall \mathbf{x} \in \Omega_t^F \tag{6}$$

$$\nabla \cdot \mathbf{v} = 0 \quad \forall t \in (0,T) \ \ \forall \mathbf{x} \in \Omega_t^F \tag{7}$$

$$\sigma^F = -p\mathbb{I} + 2\mu^F \varepsilon(\mathbf{v}) \tag{8}$$

$$\sigma^F \mathbf{n}^F = \mathbf{h}_{\text{in}} \quad \text{on } \Sigma_1 \times (0,T) \tag{9}$$

$$\sigma^F \mathbf{n}^F = \mathbf{h}_{\text{out}} \quad \text{on } \Sigma_3 \times (0,T) \tag{10}$$

$$\mathbf{v} = 0 \quad \text{on } \Sigma_2 \times (0,T) \tag{11}$$

where $\rho^F > 0$ and $\mu^F > 0$ are the mass density and the viscosity of the fluid, $\mathbf{f}^F = (f_1^F, f_2^F)$ are the applied volume forces, in general the gravity forces, $h_{\text{in}} : \Sigma_1 \times (0,T) \to \mathbb{R}$ and $h_{\text{out}} : \Sigma_3 \times (0,T) \to \mathbb{R}$ are prescribed boundary stress, $\mathbf{n}^F$ is the unit outer normal vector along the boundary $\partial\Omega_t^F$.

The interface Γ_t is the image of the boundary Γ_0 by the map

$$\mathbb{T}(\mathbf{X}) = \mathbf{X} + \mathbf{u}(\mathbf{X}, t)$$

DOI: 10.1002/fld

Interface conditions:

$$\mathbf{v}(\mathbf{X}+\mathbf{u}(\mathbf{X},t),t)=\frac{\partial \mathbf{u}}{\partial t}(\mathbf{X},t) \quad \forall(\mathbf{X},t)\in\Gamma_0\times(0,T) \tag{12}$$

$$(\sigma^{\mathrm{F}}\mathbf{n}^{\mathrm{F}})_{(\mathbf{X}+\mathbf{u}(\mathbf{X},t),t)}=-(\sigma^{\mathrm{S}}\mathbf{n}^{\mathrm{S}})_{(\mathbf{X},t)} \quad \forall(\mathbf{X},t)\in\Gamma_0\times(0,T) \tag{13}$$

Equations (12) and (13) represent the continuity of velocity and of stress at the interface, respectively.

Initial conditions:

$$\mathbf{u}(\mathbf{X},t=0)=\mathbf{u}^0(\mathbf{X}) \quad \text{in } \Omega^{\mathrm{S}} \tag{14}$$

$$\frac{\partial \mathbf{u}}{\partial t}(\mathbf{X},t=0)=\dot{\mathbf{u}}^0(\mathbf{X}) \quad \text{in } \Omega^{\mathrm{S}} \tag{15}$$

$$\mathbf{v}(\mathbf{x},t=0)=\mathbf{v}^0(\mathbf{x}) \quad \text{in } \Omega_0^{\mathrm{F}} \tag{16}$$

where $\mathbf{u}^0$ is the initial structure displacement, $\dot{\mathbf{u}}^0$ is the initial structure velocity and $\mathbf{v}^0$ is the initial fluid velocity.

The governing equations for fluid–structure interaction problem are (1)–(16). The above fluid and structure models could be considered unbalanced: on the one hand, the structure is governed by a linear elastic constitutive law adapted for small displacements and, on the other hand, the fluid equations are written in a moving domain. In the real life, the displacement of a segment of human artery (6 cm length, 0.1 cm thickness, 1 cm diameter) is about 0.1 cm, therefore a linear mathematical model for the structure could be sufficient for this particular application. Contrary to the elastic solids, the fluids are very sensitive to a moving boundary. This is probably due to weak intermolecular forces and even a small displacement of a boundary produces important modifications in a fluid flow. For this reason, it is necessary to write the fluid equations in a moving domain. Coupling Navier–Stokes equations with a linear model for the structure was used in [2, 6, 20] where the structure is governed by the independent rings model, by Navier equation [21] or by a linear membrane [22, 23].

Non-linear elasticity equations: In applications with large displacement of the structure, non-linear models have to be used as in [5, 10, 13, 18] (shells), in [24] (beams), or in [25] (membrane). In this paper, we include also the study of the interaction of the Navier–Stokes equations with a non-linear St Venant–Kirchhoff elasticity model (see [26]). We just replace Equations (2)–(3) by

$$\sigma^{\mathrm{S}}=\lambda^{\mathrm{S}}(E_{11}(\mathbf{u})+E_{22}(\mathbf{u}))\mathbb{I}+2\mu^{\mathrm{S}}\mathbb{E}(\mathbf{u}) \tag{17}$$

$$\mathbb{E}(\mathbf{u})=\tfrac{1}{2}(\nabla\mathbf{u}+(\nabla\mathbf{u})^{\mathrm{T}}+(\nabla\mathbf{u})^{\mathrm{T}}\nabla\mathbf{u}) \tag{18}$$

where $\mathbb{E}(\mathbf{u})=(E_{ij}(\mathbf{u}))_{i,j=1,2}$, is the Green–St Venant strain tensor. The non-linear St Venant–Kirchhoff elasticity model could be used for large displacements but small strains of the structure.

3. STRUCTURE APPROXIMATION BY CENTERED TIME ADVANCING SCHEME

We introduce the following Hilbert space:

$$\mathbf{W}^{\mathrm{S}}=\{\mathbf{w}^{\mathrm{S}}\in(H^1(\Omega^{\mathrm{S}}))^2;\ \mathbf{w}^{\mathrm{S}}=0 \text{ on } \Gamma_{\mathrm{D}}\}$$

DOI: 10.1002/fld

The habitual regularity of a weak solution of the linear elasticity model is $u \in L^2(0,T;\mathbf{W}^{\mathrm{S}})$ and $\mathrm{d}u/\mathrm{d}t \in L^2(0,T;(H^1(\Omega^{\mathrm{S}}))^2)$ (see [27, Chapter XVIII]), but for fluid–structure interaction problem, more regularity is required (see [28]). For example, condition (12) makes sense if the structure velocity $\mathrm{d}u/\mathrm{d}t(t)$ is at least in $(H^1(\Omega^{\mathrm{S}}))^2$.

Multiplying Equation (1) by $\mathbf{w}^{\mathrm{S}} \in \mathbf{W}^{\mathrm{S}}$ and from the Green formula, we obtain

$$\int_{\Omega^{\mathrm{S}}} \rho^{\mathrm{S}} \frac{\partial^2 \mathbf{u}}{\partial t^2} \cdot \mathbf{w}^{\mathrm{S}} \,\mathrm{d}\mathbf{X} + a_{\mathrm{S}}(\mathbf{u}, \mathbf{w}^{\mathrm{S}}) = \int_{\Omega^{\mathrm{S}}} \mathbf{f}^{\mathrm{S}} \cdot \mathbf{w}^{\mathrm{S}} \,\mathrm{d}\mathbf{X} + \int_{\Gamma_0} (\sigma^{\mathrm{S}} \mathbf{n}^{\mathrm{S}}) \cdot \mathbf{w}^{\mathrm{S}} \,\mathrm{d}s \quad \forall \mathbf{w}^{\mathrm{S}} \in \mathbf{W}^{\mathrm{S}} \tag{19}$$

where

$$a_{\mathrm{S}}(\mathbf{u}, \mathbf{w}^{\mathrm{S}}) = \int_{\Omega^{\mathrm{S}}} \lambda^{\mathrm{S}} (\nabla \cdot \mathbf{u})(\nabla \cdot \mathbf{w}^{\mathrm{S}}) \,\mathrm{d}\mathbf{X} + \int_{\Omega^{\mathrm{S}}} 2\mu^{\mathrm{S}} \varepsilon(\mathbf{u}) : \varepsilon(\mathbf{w}^{\mathrm{S}}) \,\mathrm{d}\mathbf{X}$$

in the linear case and

$$a_{\mathrm{S}}(\mathbf{u}, \mathbf{w}^{\mathrm{S}}) = \int_{\Omega^{\mathrm{S}}} (\lambda^{\mathrm{S}} (E_{11}(\mathbf{u}) + E_{22}(\mathbf{u}))\mathbb{I} + 2\mu^{\mathrm{S}} \mathbb{E}(\mathbf{u})) : (\nabla \mathbf{w}^{\mathrm{S}}) \,\mathrm{d}\mathbf{X}$$

in the non-linear case.

3.1. Modal decomposition of the linear model

For each $i \in \mathbb{N}^*$, there exists an unique eigenvalue $\lambda_i > 0$ and an unique eigenfunction $\boldsymbol{\phi}^i \in \mathbf{W}^{\mathrm{S}}$, solution of

$$a_{\mathrm{S}}(\boldsymbol{\phi}^i, \mathbf{w}^{\mathrm{S}}) = \lambda_i \int_{\Omega^{\mathrm{S}}} \rho^{\mathrm{S}} \boldsymbol{\phi}^i \cdot \mathbf{w}^{\mathrm{S}} \mathrm{d}\mathbf{X} \quad \forall \mathbf{w}^{\mathrm{S}} \in \mathbf{W}^{\mathrm{S}} \tag{20}$$

such that

$$\int_{\Omega^{\mathrm{S}}} \rho^{\mathrm{S}} \boldsymbol{\phi}^i \cdot \boldsymbol{\phi}^j \,\mathrm{d}\mathbf{X} = \delta_{ij} \tag{21}$$

Let us denote by $\alpha_i(t) = \int_{\Gamma_0} (\sigma^{\mathrm{S}} \mathbf{n}^{\mathrm{S}})(t) \cdot \boldsymbol{\phi}^i \,\mathrm{d}s$. The problem (19) has a solution of the form

$$\mathbf{u}(t) = \sum_{i \geqslant 1} q_i(t) \boldsymbol{\phi}^i$$

where q_i is the solution of the second-order differential equation

$$q_i''(t) + \lambda_i q_i(t) = \int_{\Omega^{\mathrm{S}}} \mathbf{f}^{\mathrm{S}}(t) \cdot \boldsymbol{\phi}^i \,\mathrm{d}\mathbf{X} + \alpha_i(t), \quad t \in (0,T) \tag{22}$$

$$q_i(0) = \int_{\Omega^{\mathrm{S}}} \rho^{\mathrm{S}} \mathbf{u}^0 \cdot \boldsymbol{\phi}^i \,\mathrm{d}\mathbf{X} \tag{23}$$

$$q_i'(0) = \int_{\Omega^{\mathrm{S}}} \rho^{\mathrm{S}} \dot{\mathbf{u}}^0 \cdot \boldsymbol{\phi}^i \,\mathrm{d}\mathbf{X} \tag{24}$$

The solution of problem (20)–(21) can be approached by using the finite element method. We have to solve in this case a generalized eigenproblem of the form

$$K_h \boldsymbol{\Phi}_h^i = \lambda_{i,h} M_h \boldsymbol{\Phi}_h^i, \quad (\boldsymbol{\Phi}_h^j)^{\mathrm{T}} M_h \boldsymbol{\Phi}_h^i = \mathbb{I}$$

DOI: 10.1002/fld

Remark 1
Following [29, p. 572], when the initial displacement and velocity are zero, the solution of (22) is given by

$$q_i(t)=\frac{1}{\sqrt{\lambda_i}}\int_0^t f_i(s)\sin(\sqrt{\lambda_i}(t-s))\,\mathrm{d}s$$

where $f_i(t)=\int_{\Omega^S}\mathbf{f}^S(t)\cdot\boldsymbol{\phi}^i\,\mathrm{d}\mathbf{X}+\alpha_i(t)$. If λ_i is very large, the influence of $q_i(t)$ in $\mathbf{u}(t)$ diminishes, therefore in practical calculation, only the first m eigenvalues will be considered

$$0<\lambda_{1,h}\leqslant\lambda_{2,h}\leqslant\cdots\leqslant\lambda_{m,h}$$

Let $N\in\mathbb{N}^*$ be the number of time steps and $\Delta t=T/N$ the time step. We set $t_n=n\Delta t$ for $n=0,1,\ldots,N$. We denote $\alpha_i^n=\alpha_i(t_n)$ and let q_i^n be approximation of $q_i(t_n)$.

Equation (22) will be approached by the following centered scheme: knowing q_i^{n-1} and q_i^n, find q_i^{n+1} such that

$$\begin{aligned}&\frac{(q_i^{n+1}-2q_i^n+q_i^{n-1})}{(\Delta t)^2}+\lambda_{i,h}(\theta q_i^{n+1}+(1-2\theta)q_i^n+\theta q_i^{n-1})\\&\quad=\int_{\Omega^S}(\theta\mathbf{f}^{S,n+1}+(1-2\theta)\mathbf{f}^{S,n}+\theta\mathbf{f}^{S,n-1})\cdot\boldsymbol{\phi}^i\,\mathrm{d}\mathbf{X}+\theta\alpha_i^{n+1}+(1-2\theta)\alpha_i^n+\theta\alpha_i^{n-1}\end{aligned}\tag{25}$$

where θ is a real parameter in $(0,\frac{1}{2})$ and $\mathbf{f}^{S,n}=\mathbf{f}^S(t_n)$ are the volume forces. This scheme is of second order in time and if $\theta\in[\frac{1}{4},\frac{1}{2}]$, then it is unconditionally stable.

The structure displacement at time instant t_n will be approached by

$$\mathbf{u}_h^n(\mathbf{X})=\sum_{i=1}^m q_i^n\boldsymbol{\phi}_h^i(\mathbf{X})\quad\forall\mathbf{X}\in\Omega^S$$

3.2. Newton's method for the non-linear model

A second-order time advancing scheme for (19) is: find $\mathbf{u}^{n+1}\in\mathbf{W}^S$ an approximation of $\mathbf{u}(t_{n+1})$ such that

$$\begin{aligned}&\int_{\Omega^S}\rho^S\frac{(\mathbf{u}^{n+1}-2\mathbf{u}^n+\mathbf{u}^{n-1})}{(\Delta t)^2}\cdot\mathbf{w}^S\,\mathrm{d}\mathbf{X}\\&\qquad+\theta a_S(\mathbf{u}^{n+1},\mathbf{w}^S)+(1-2\theta)a_S(\mathbf{u}^n,\mathbf{w}^S)+\theta a_S(\mathbf{u}^{n-1},\mathbf{w}^S)\\&\quad=\int_{\Omega^S}(\theta\mathbf{f}^{S,n+1}+(1-2\theta)\mathbf{f}^{S,n}+\theta\mathbf{f}^{S,n-1})\cdot\mathbf{w}^S\,\mathrm{d}\mathbf{X}\\&\qquad+\int_{\Gamma_0}(\theta\mathbf{F}^{S,n+1}+(1-2\theta)\mathbf{F}^{S,n}+\theta\mathbf{F}^{S,n-1})\cdot\mathbf{w}^S\,\mathrm{d}s\quad\forall\mathbf{w}^S\in\mathbf{W}^S\end{aligned}\tag{26}$$

where $\mathbf{f}^{S,n}=\mathbf{f}^S(t_n)$ are the volume forces, $\mathbf{F}^{S,n}=(\sigma^S\mathbf{n}^S)(t_n)$ are the surface forces acting on the interface and θ is a real parameter in $(0,\frac{1}{2})$.

DOI: 10.1002/fld

We recall that the components of the St Venant–Kirchhoff stress tensor are

$$\sigma_{ij}^{\mathrm{S}}(\mathbf{u})=\lambda^{\mathrm{S}}(E_{11}(\mathbf{u})+E_{22}(\mathbf{u}))\delta_{ij}+2\mu^{\mathrm{S}}E_{ij}(\mathbf{u})$$

where the Green–St Venant strain tensor $\mathbb{E}(\mathbf{u})$ is given by (18). The map $\mathbf{u}\to\mathbb{E}(\mathbf{u})$ is non-linear and we will use the Newton's method in order to obtain $\mathbf{u}^{n+1}$ the solution of (26).

Knowing the derivative with respect to $\mathbf{u}$ of the components of the Green–St Venant strain tensor for an arbitrary $\mathbf{h}=(h_1,h_2)$ in $\mathbf{W}^{\mathrm{S}}$,

$$\frac{\mathrm{d}E_{11}}{\mathrm{d}\mathbf{u}}(\mathbf{u})\mathbf{h}=\frac{1}{2}\left(2\frac{\partial h_1}{\partial x_1}+2\frac{\partial u_1}{\partial x_1}\frac{\partial h_1}{\partial x_1}+2\frac{\partial u_1}{\partial x_2}\frac{\partial h_1}{\partial x_2}\right)$$

$$\frac{\mathrm{d}E_{22}}{\mathrm{d}\mathbf{u}}(\mathbf{u})\mathbf{h}=\frac{1}{2}\left(2\frac{\partial h_2}{\partial x_2}+2\frac{\partial u_2}{\partial x_1}\frac{\partial h_2}{\partial x_1}+2\frac{\partial u_2}{\partial x_2}\frac{\partial h_2}{\partial x_2}\right)$$

$$\frac{\mathrm{d}E_{12}}{\mathrm{d}\mathbf{u}}(\mathbf{u})\mathbf{h}=\frac{1}{2}\left(\frac{\partial h_1}{\partial x_2}+\frac{\partial h_2}{\partial x_1}+\frac{\partial u_2}{\partial x_1}\frac{\partial h_1}{\partial x_1}+\frac{\partial u_2}{\partial x_2}\frac{\partial h_1}{\partial x_2}+\frac{\partial u_1}{\partial x_1}\frac{\partial h_2}{\partial x_1}+\frac{\partial u_1}{\partial x_2}\frac{\partial h_2}{\partial x_2}\right)$$

$$\frac{\mathrm{d}E_{21}}{\mathrm{d}\mathbf{u}}(\mathbf{u})\mathbf{h}=\frac{\mathrm{d}E_{12}}{\mathrm{d}\mathbf{u}}(\mathbf{u})\mathbf{h}$$

we can compute easily

$$\frac{\mathrm{d}a_{\mathrm{S}}}{\mathrm{d}\mathbf{u}}(\mathbf{u},\mathbf{w}^{\mathrm{S}})\mathbf{h}=\sum_{i,j=1}^{2}\int_{\Omega^{\mathrm{S}}}\frac{\mathrm{d}\sigma_{ij}^{\mathrm{S}}}{\mathrm{d}\mathbf{u}}(\mathbf{u})\mathbf{h}\frac{\partial w_i^{\mathrm{S}}}{\partial x_j}\,\mathrm{d}\mathbf{X}$$

Newton's method for solving (26)

Step 0: Initialization. Set $k=0$ and $\mathbf{u}^{n+1,0}=\mathbf{u}^n$. We will generate $\mathbf{u}^{n+1,k}$ for $k=1,2,\ldots$.

Step 1: Find $\mathbf{h}^k$ the solution of the linear system

$$\begin{aligned}
&\int_{\Omega^{\mathrm{S}}}\rho^{\mathrm{S}}\frac{\mathbf{h}^k}{(\Delta t)^2}\cdot\mathbf{w}^{\mathrm{S}}\,\mathrm{d}\mathbf{X}+\frac{\mathrm{d}a_{\mathrm{S}}}{\mathrm{d}\mathbf{u}}(\mathbf{u}^{n+1,k},\mathbf{w}^{\mathrm{S}})\mathbf{h}^k\\
&\quad=\int_{\Omega^{\mathrm{S}}}\rho^{\mathrm{S}}\frac{(\mathbf{u}^{n+1,k}-2\mathbf{u}^n+\mathbf{u}^{n-1})}{(\Delta t)^2}\cdot\mathbf{w}^{\mathrm{S}}\,\mathrm{d}\mathbf{X}\\
&\qquad+\theta a_{\mathrm{S}}(\mathbf{u}^{n+1,k},\mathbf{w}^{\mathrm{S}})+(1-2\theta)a_{\mathrm{S}}(\mathbf{u}^n,\mathbf{w}^{\mathrm{S}})+\theta a_{\mathrm{S}}(\mathbf{u}^{n-1},\mathbf{w}^{\mathrm{S}})\\
&\qquad-\int_{\Omega^{\mathrm{S}}}(\theta\mathbf{f}^{\mathrm{S},n+1}+(1-2\theta)\mathbf{f}^{\mathrm{S},n}+\theta\mathbf{f}^{\mathrm{S},n-1})\cdot\mathbf{w}^{\mathrm{S}}\mathrm{d}\mathbf{X}\\
&\qquad-\int_{\Gamma_0}(\theta\mathbf{F}^{\mathrm{S},n+1}+(1-2\theta)\mathbf{F}^{\mathrm{S},n}+\theta\mathbf{F}^{\mathrm{S},n-1})\cdot\mathbf{w}^{\mathrm{S}}\,\mathrm{d}s\quad\forall\mathbf{w}^{\mathrm{S}}\in\mathbf{W}^{\mathrm{S}}
\end{aligned}\tag{27}$$

Step 2: If $\mathbf{h}^k$ is small, then stop.

Step 3: Set $\mathbf{u}^{n+1,k+1}=\mathbf{u}^{n+1,k}-\mathbf{h}^k$; $k\leftarrow k+1$; go to *Step 1*.

The variational equation (27) will be solved by the finite element method. We denote by $\mathbf{u}_h^{n+1}$ the displacement of the structure at the time instant t_{n+1}.

DOI: 10.1002/fld

4. ARBITRARY LAGRANGIAN EULERIAN (ALE) FRAMEWORK FOR APPROXIMATION OF FLUID EQUATIONS

Let $\widehat{\Omega}^{\mathrm{F}}$ be a reference fixed domain. Let $\mathscr{A}_t$, $t\in[0,T]$ be a family of transformations such that $\mathscr{A}_t(\widehat{\mathbf{x}})=\widehat{\mathbf{x}}$, $\forall\widehat{\mathbf{x}}\in\Sigma_1\cup\Sigma_2\cup\Sigma_3$, $\mathscr{A}_t(\Gamma_0)=\Gamma_t$, $\mathscr{A}_t(\widehat{\Omega}^{\mathrm{F}})=\Omega_t^{\mathrm{F}}$, where $\widehat{\mathbf{x}}=(\widehat{x}_1,\widehat{x}_2)^{\mathrm{T}}\in\widehat{\Omega}^{\mathrm{F}}$ represent the ALE coordinates and $\mathbf{x}=(x_1,x_2)^{\mathrm{T}}=\mathscr{A}_t(\widehat{\mathbf{x}})$ the Eulerian coordinates.

Let v be the velocity of the fluid in the Eulerian coordinates. The corresponding function in the ALE framework $\widehat{v}:\widehat{\Omega}^{\mathrm{F}}\times[0,T]\to\mathbb{R}^2$ is defined by $\widehat{v}(\widehat{\mathbf{x}},t)=v(\mathscr{A}_t(\widehat{\mathbf{x}}),t)=v(\mathbf{x},t)$. We denote the ALE time derivative by $\partial v/\partial t|_{\widehat{\mathbf{x}}}(\mathbf{x},t)=\partial\widehat{v}/\partial t(\widehat{\mathbf{x}},t)$ and the domain velocity by $\boldsymbol{\vartheta}(\mathbf{x},t)=\partial\mathscr{A}_t/\partial t(\widehat{\mathbf{x}})$.

In order to obtain the existence of a weak solution of the Navier–Stokes equations in moving domain, we assume that $\mathbf{v}(t)\in(H^1(\Omega_t^{\mathrm{F}}))^2$, $p(t)\in L^2(\Omega_t^{\mathrm{F}})$ and $\mathscr{A}_t$ is $\mathscr{C}^1$-diffeomorphism for each t, but for fluid–structure interaction problem, the existence is obtained in some particular Sobolev spaces (see [28]).

The Navier–Stokes equations in the ALE framework give: find the fluid velocity $\mathbf{v}$ verifying (12) and the fluid pressure p such that

$$\rho^{\mathrm{F}}\left(\left.\frac{\partial\mathbf{v}}{\partial t}\right|_{\widehat{\mathbf{x}}}+((\mathbf{v}-\boldsymbol{\vartheta})\cdot\nabla)\mathbf{v}\right)-2\mu^{\mathrm{F}}\nabla\cdot\varepsilon(\mathbf{v})+\nabla p=\mathbf{f}^{\mathrm{F}}\quad\forall t\in(0,T)\ \ \forall\mathbf{x}\in\Omega_t^{\mathrm{F}}$$

$$\nabla\cdot\mathbf{v}=0\quad\forall t\in(0,T)\ \ \forall\mathbf{x}\in\Omega_t^{\mathrm{F}}$$

Multiplying the above equations by $\mathbf{w}^{\mathrm{F}}$ and q, respectively, and using the Green formula, we have

$$\int_{\Omega_t^{\mathrm{F}}}\rho^{\mathrm{F}}\left.\frac{\partial\mathbf{v}}{\partial t}\right|_{\widehat{\mathbf{x}}}\cdot\mathbf{w}^{\mathrm{F}}\,\mathrm{d}\mathbf{x}+\int_{\Omega_t^{\mathrm{F}}}\rho^{\mathrm{F}}(((\mathbf{v}-\boldsymbol{\vartheta})\cdot\nabla)\mathbf{v})\cdot\mathbf{w}^{\mathrm{F}}\,\mathrm{d}\mathbf{x}$$

$$+a_{\mathrm{F}}(\mathbf{v},\mathbf{w}^{\mathrm{F}})+b_{\mathrm{F}}(\mathbf{w}^{\mathrm{F}},p)=\ell_{\mathrm{F}}(\mathbf{w}^{\mathrm{F}})\quad\forall\mathbf{w}^{\mathrm{F}}=0\quad\text{on }\Sigma_2\cup\Gamma_t$$

$$b_{\mathrm{F}}(\mathbf{v},q)=0\quad\forall q$$

where

$$a_{\mathrm{F}}(\mathbf{v},\mathbf{w}^{\mathrm{F}})=\int_{\Omega_t^{\mathrm{F}}}2\mu^{\mathrm{F}}\varepsilon(\mathbf{v}):\varepsilon(\mathbf{w}^{\mathrm{F}})\,\mathrm{d}\mathbf{x}$$

$$b_{\mathrm{F}}(\mathbf{w}^{\mathrm{F}},q)=-\int_{\Omega_t^{\mathrm{F}}}(\nabla\cdot\mathbf{w}^{\mathrm{F}})q\,\mathrm{d}\mathbf{x}$$

$$\ell_{\mathrm{F}}(\mathbf{w}^{\mathrm{F}})=\int_{\Omega_t^{\mathrm{F}}}\mathbf{f}^{\mathrm{F}}\cdot\mathbf{w}^{\mathrm{F}}\,\mathrm{d}\mathbf{x}+\int_{\Sigma_1}\mathbf{h}_{\mathrm{in}}\cdot\mathbf{w}^{\mathrm{F}}\,\mathrm{d}s+\int_{\Sigma_3}\mathbf{h}_{\mathrm{out}}\cdot\mathbf{w}^{\mathrm{F}}\,\mathrm{d}s$$

For the approximation of fluid equations, we employ a time integration algorithm based on the backward Euler scheme and a semi-implicit treatment of the convection term. In the case of a fixed domain, this scheme has been analyzed in [30], where the unconditional stability is proved. For the fully discrete problem in a fixed domain, a stability bound on $\Delta t/h^{\alpha}$ is required, where $\alpha>0$. This condition is less restrictive than the condition necessary for the explicit algorithm.

Knowing Ω_n^{F}, $\Omega_{n+1}^{\mathrm{F}}$, $\mathbf{V}^n$, $\boldsymbol{\vartheta}^{n+1}$, find $\mathbf{v}^{n+1}$ and p^{n+1} such that

$$\mathbf{v}^{n+1}(\mathbf{X}+\mathbf{u}_h^{n+1}(\mathbf{X}))=\sum_{i=1}^{m}\frac{q_i^{n+1}-q_i^n}{\Delta t}\boldsymbol{\phi}_h^i(\mathbf{X})\quad\forall\mathbf{X}\in\Gamma_0\tag{28}$$

DOI: 10.1002/fld

$$\int_{\Omega^{\mathrm{F}}_{n+1}} \rho^{\mathrm{F}} \left(\frac{\mathbf{v}^{n+1} - \mathbf{V}^n}{\Delta t} \right) \cdot \mathbf{w}^{\mathrm{F}} \, \mathrm{d}\mathbf{x} + \int_{\Omega^{\mathrm{F}}_{n+1}} \rho^{\mathrm{F}} (((\mathbf{V}^n - \vartheta^{n+1}) \cdot \nabla) \mathbf{v}^{n+1}) \cdot \mathbf{w}^{\mathrm{F}} \, \mathrm{d}\mathbf{x}$$

$$+ \int_{\Omega^{\mathrm{F}}_{n+1}} 2\mu^{\mathrm{F}} \varepsilon(\mathbf{v}^{n+1}) : \varepsilon(\mathbf{w}^{\mathrm{F}}) \, \mathrm{d}\mathbf{x} - \int_{\Omega^{\mathrm{F}}_{n+1}} (\nabla \cdot \mathbf{w}^{\mathrm{F}}) \, p^{n+1} \, \mathrm{d}\mathbf{x}$$

$$= \int_{\Omega^{\mathrm{F}}_{n+1}} \mathbf{f}^{\mathrm{F}} \cdot \mathbf{w}^{\mathrm{F}} \, \mathrm{d}\mathbf{x} + \int_{\Sigma_1} \mathbf{h}^{n+1}_{\mathrm{in}} \cdot \mathbf{w}^{\mathrm{F}} \, \mathrm{d}s + \int_{\Sigma_3} \mathbf{h}^{n+1}_{\mathrm{out}} \cdot \mathbf{w}^{\mathrm{F}} \, \mathrm{d}s \quad \forall \mathbf{w}^{\mathrm{F}} = 0 \quad \text{on } \Sigma_2 \cup \Gamma_{n+1} \tag{29}$$

$$- \int_{\Omega^{\mathrm{F}}_{n+1}} (\nabla \cdot \mathbf{v}^{n+1}) q \, \mathrm{d}\mathbf{x} = 0 \quad \forall q \tag{30}$$

where

$$\mathbf{V}^n(\mathbf{x}) = \mathbf{v}^n(\mathscr{A}_{t_n} \circ \mathscr{A}^{-1}_{t_{n+1}}(\mathbf{x})) \quad \text{and} \quad \vartheta^{n+1}(\mathbf{x}) = \frac{\mathscr{A}_{t_{n+1}}(\widehat{\mathbf{x}}) - \mathscr{A}_{t_n}(\widehat{\mathbf{x}})}{\Delta t} = \frac{\mathbf{x} - \mathscr{A}_{t_n} \circ \mathscr{A}^{-1}_{t_{n+1}}(\mathbf{x})}{\Delta t}$$

The condition (28) is the discrete version of the continuity of the velocity at the interface (12).

Building the discrete ALE map

Let $\mathscr{T}^0_h$ be a mesh of triangular finite elements for the reference domain $\widehat{\Omega}^{\mathrm{F}} = \Omega^{\mathrm{F}}_0$.

If we know the displacement of the structure $\widetilde{\mathbf{u}}^{n+1}_h : \Omega^{\mathrm{S}} \to \mathbb{R}^2$, we can compute $\widetilde{\mathbf{d}}^{n+1} : \Omega^{\mathrm{F}}_0 \to \mathbb{R}^2$ from the following boundary value problem:

$$\Delta \widetilde{\mathbf{d}}^{n+1} = 0 \quad \text{on } \Omega^{\mathrm{F}}_0 \tag{31}$$

$$\widetilde{\mathbf{d}}^{n+1} = \widetilde{\mathbf{u}}^{n+1}_h \quad \text{on } \Gamma_0 \tag{32}$$

$$\widetilde{\mathbf{d}}^{n+1} = 0 \quad \text{on } \Sigma_1 \cup \Sigma_2 \cup \Sigma_3 \tag{33}$$

We can set the discrete ALE map as follows $\mathscr{A}_{h,n+1}(\widehat{\mathbf{x}}) = \widehat{\mathbf{x}} + \widetilde{\mathbf{d}}^{n+1}(\widehat{\mathbf{x}})$ and the mesh for the domain at time instant t_{n+1} can be obtained by

$$\widetilde{\mathscr{T}}^{n+1}_h = \mathscr{A}_{h,n+1}(\mathscr{T}^0_h) \tag{34}$$

Sometimes, especially for non-convex domains, the ALE map obtained by harmonic extension reverses the triangles of the reference domain and produces non-valid mesh. An alternative technique is to minimize the energy of a mechanical system formed by a set of springs that joins the mesh nodes. A penalty term could ensure that the triangles are not reversed.

The mesh velocity is computed by the finite difference formula

$$\widetilde{\vartheta}^{n+1}(\mathbf{x}) = \frac{\widetilde{\mathbf{d}}^{n+1}(\widehat{\mathbf{x}}) - \widetilde{\mathbf{d}}^{n}(\widehat{\mathbf{x}})}{\Delta t} \tag{35}$$

If we predict explicitly the structure displacement by the formula $\widetilde{\mathbf{u}}^{n+1}_h = 2\mathbf{u}^n_h - \mathbf{u}^{n-1}_h$, we can obtain directly the mesh velocity as the solution of

$$\Delta \widetilde{\vartheta}^{n+1} = 0 \quad \text{on } \Omega^{\mathrm{F}}_0$$

$$\widetilde{\vartheta}^{n+1} = \frac{2\mathbf{u}^n_h - 3\mathbf{u}^{n-1}_h + \mathbf{u}^{n-2}_h}{\Delta t} \quad \text{on } \Gamma_0$$

$$\widetilde{\vartheta}^{n+1} = 0 \quad \text{on } \Sigma_1 \cup \Sigma_2 \cup \Sigma_3$$

DOI: 10.1002/fld

Now, the right side part of the boundary condition on Γ_0 depends on the displacements of the structure obtained after solving the coupled problem at previous time steps. Other possibility used in [18] is to prescribe the mesh velocity at the interface to be $3\dot{\mathbf{u}}_h^n - \dot{\mathbf{u}}_h^{n-1}/2$ which is Adams–Bashforth formula. We have denoted by $\dot{\mathbf{u}}_h^n$ an approximation of the structure velocity at time instant t_n. Also, we can use higher order multi-step backward extrapolating schemes.

5. IMPLICIT AND SEMI-IMPLICIT TIME INTEGRATION SCHEMES

The method that we use here to solve the coupled problem uses partitioned procedure (the fluid and structure equations are solved separately), which is very often used technique to solve fluid–structure interaction problems. In this way, the exiting solvers for each problem can be employed. Alternatively, the fluid–structure interaction problems could be solved by monolithic algorithms [31].

At each time step, an optimization problem of the form

$$\inf_{\boldsymbol{\alpha}\in\mathbb{R}^m} J(\boldsymbol{\alpha})$$

has to be solved. This technique was successfully employed in [16, 17], where implicit algorithms are presented. We will use the same least square method based on the BFGS method in order to impose the continuity of the stress at the interface. Details on the BFGS algorithm can be found in [32].

5.1. The structure is governed by a linear model and solved by modal decomposition

In a previous section, we have denoted by

$$\alpha_i(t) = \int_{\Gamma_0} (\sigma^{\mathrm{S}}\mathbf{n}^{\mathrm{S}})(t)\cdot\boldsymbol{\phi}^i \,\mathrm{d}s$$

The stress at the fluid–structure interface $(\sigma^{\mathrm{S}}\mathbf{n}^{\mathrm{S}})(t)$ is not known. Since the stress is continuous across the interface, we obtain that

$$\int_{\Gamma_0} (\sigma^{\mathrm{S}}\mathbf{n}^{\mathrm{S}})(t)\cdot\boldsymbol{\phi}^i \,\mathrm{d}s = -\int_{\Gamma_0} (\sigma^{\mathrm{F}}\mathbf{n}^{\mathrm{F}})_{(\mathbf{X}+\mathbf{u}(\mathbf{X},t),t)}\cdot\boldsymbol{\phi}^i \,\mathrm{d}s$$

Consequently, if we set

$$\beta_i(t) = -\int_{\Gamma_0} (\sigma^{\mathrm{F}}\mathbf{n}^{\mathrm{F}})_{(\mathbf{X}+\mathbf{u}(\mathbf{X},t),t)}\cdot\boldsymbol{\phi}^i \,\mathrm{d}s \tag{36}$$

we get $\alpha_i(t) = \beta_i(t)$, for all $i \geqslant 1$ and $t \in [0, T]$. After the full discretization, this equality does not hold and it will be treated by the least-squares method.

How the stress at the fluid–structure interface is computed

Method 1: The integral (36) mixes functions defined on different domains: the fluid stress tensor defined in the fluid domain, the unit outer normal vector defined on the interface and an eigenfunction defined in the structure domain. If $\mathbf{v}_h$ and p_h are finite element approximations of fluid velocity and pressure, respectively, we can define σ_h^{F} the $\mathbb{P}_1$ interpolation of $-p_h\mathbb{I} + 2\mu^{\mathrm{F}}\varepsilon(\mathbf{v}_h)$.

DOI: 10.1002/fld

On every segment of the interface, we can compute the normal $\mathbf{n}_h^{\mathrm{F}}$. Let us define $\mathbf{g}_h = \sigma_h^{\mathrm{F}} \mathbf{n}_h^{\mathrm{F}}$, which is a piecewise linear function on the interface, but not continuous. Without supplementary computations, we set $\widehat{\mathbf{g}}_h(\mathbf{X}, t) = \mathbf{g}_h(\mathbf{X} + \mathbf{u}_h(\mathbf{X}, t), t)$. More precisely, in a node $\mathbf{P}$ of the mesh of Γ_0, the finite element function $\widehat{\mathbf{g}}_h$ takes the same value as $\mathbf{g}_h$ in the node $\mathbf{P} + \mathbf{u}_h(\mathbf{P}, t)$ of the mesh of Γ_t. Though both the finite element functions $\widehat{\mathbf{g}}_h$ and $\boldsymbol{\phi}_h^i$ are defined on Γ_0, the first one use a grid derived from the fluid mesh and the other use the structure mesh, which are not necessarily compatible at the interface. Finally, we compute

$$\beta_i(t) = -\int_{\Gamma_0} \widehat{\mathbf{g}}_h \cdot \boldsymbol{\phi}_h^i \, \mathrm{d}s$$

Method 2: Alternatively, we can approach $\beta_i(t)$ by

$$-\int_{\Gamma_t} (\sigma_h^{\mathrm{F}} \mathbf{n}_h^{\mathrm{F}}) \cdot \boldsymbol{\phi}_h^i (\mathbb{T}^{-1}) \, \mathrm{d}s$$

Method 3: Let us introduce the fluid stress tensor defined on the reference domain $\widehat{\Omega}^{\mathrm{F}}$ of components

$$\widehat{\Sigma}_{ij}^{\mathrm{F}} = -\widehat{p}\,\delta_{ij} + \mu^{\mathrm{F}} \left(\frac{\partial \widehat{v}_i}{\partial \widehat{x}_j} + \frac{\partial \widehat{v}_j}{\partial \widehat{x}_i} \right)$$

We can approach $\beta_i(t)$ by

$$-\int_{\Gamma_0} (\widehat{\Sigma}^{\mathrm{F}} \widehat{\mathbf{n}}^{\mathrm{F}}) \cdot \boldsymbol{\phi}^i \, \mathrm{d}s$$

Contrary to the first two methods, where $\mathbf{n}^{\mathrm{F}}$ have to be computed on the moving interface, the third one requires the computation of $\widehat{\mathbf{n}}^{\mathrm{F}}$ on the reference interface.

Method 4: In [33] was introduced a technique which is popular because the computation of the normal vector to the interface is not necessary. The structure load is computed as the residual of the first fluid equation.

We have employed for the numerical simulation the second and the third methods, which are more adapted to our computational environment.

Implicit time advancing algorithm

Suppose that at the previous time steps we know: $\boldsymbol{\alpha}^{n-1}, \boldsymbol{\alpha}^n \in \mathbb{R}^m$ and $\mathbf{q}^{n-1}, \mathbf{q}^n \in \mathbb{R}^m$.

Step 1: Solve by BFGS method starting from the point $\boldsymbol{\alpha}^n$ the optimization problem

$$\boldsymbol{\alpha}^{n+1} \in \arg\min_{\boldsymbol{\alpha} \in \mathbb{R}^m} J(\boldsymbol{\alpha})$$

where the cost function is computed as following:

(i) Solve the structure problem. We obtain $\mathbf{q}^{n+1}$ from (25), where $\boldsymbol{\alpha}^{n+1}$ was replaced by $\boldsymbol{\alpha}$. Then set the displacement of the structure $\mathbf{u} = \sum_{i=1}^m q_i^{n+1} \boldsymbol{\phi}^i$.
(ii) Build a fluid mesh $\mathscr{T}$ depending on the displacement $\mathbf{u}$.
(iii) Solve the fluid problem on the mesh $\mathscr{T}$ under prescribed velocity at the fluid–structure interface in order to get the fluid velocity $\mathbf{v}$ and pressure p.
(iv) Compute β_i from (36) for $i = 1, \ldots, m$.
(v) Set the cost function

$$J(\boldsymbol{\alpha}) = \tfrac{1}{2} \|\boldsymbol{\alpha} - \boldsymbol{\beta}\|_{\mathbb{R}^m}^2$$

DOI: 10.1002/fld

Step 2: Save the mesh $\mathscr{T}^{n+1}$, the structure displacement $\mathbf{u}^{n+1}$, the fluid velocity $\mathbf{v}^{n+1}$, the fluid pressure p^{n+1} obtained at the last iteration of the BFGS algorithm at *Step 1*.

Remark 2
We emphasize that in the implicit strategy, the fluid mesh changes at each call of the cost function during the minimization process. Consequently, the fluid matrix at the step (iii) have to be assembled and factorized at every cost function call.

Now, let us introduce the semi-implicit algorithm. The term 'semi-implicit' means that the interface position is computed explicitly, while the displacement of the structure, velocity and the pressure of the fluid are computed implicitly. This kind of algorithm was introduced in [18]. Our algorithm propose a different strategy based on the least-squares method in order to get the continuity of the stress at the fluid–structure interface. Also, the continuity of the velocity at the interface holds each at time step.

Semi-implicit time advancing algorithm

Step 1: Explicit prediction. Set $\widetilde{\mathbf{u}}_h^{n+1}=2\mathbf{u}_h^n-\mathbf{u}_h^{n-1}$.

Step 2: Harmonic extension. Solve $\Delta\widetilde{\mathbf{d}}^{n+1}=0$ in Ω_0^{F}, $\widetilde{\mathbf{d}}^{n+1}=\widetilde{\mathbf{u}}^{n+1}$ on Γ_0, $\widetilde{\mathbf{d}}^{n+1}=0$ on $\Sigma_1\cup\Sigma_2\cup\Sigma_3$.

Step 3: Build mesh. Set $\mathscr{A}_{h,n+1}(\widehat{\mathbf{x}})=\widehat{\mathbf{x}}+\widetilde{\mathbf{d}}^{n+1}(\widehat{\mathbf{x}})$. The mesh for the fluid domain at time instant t_{n+1} can be obtained by $\widetilde{\mathscr{T}}_h^{n+1}=\mathscr{A}_{h,n+1}(\mathscr{T}_h^0)$.

Step 4: Set the mesh velocity $\widetilde{\boldsymbol{\vartheta}}^{n+1}(\mathbf{x})=(\widetilde{\mathbf{d}}^{n+1}(\widehat{\mathbf{x}})-\widetilde{\mathbf{d}}^{n}(\widehat{\mathbf{x}}))/\Delta t$.

Step 5: Assembling the finite element matrix of fluid problem (29)–(30). Get a LU factorization of this matrix.

Step 6: Solve fluid–structure coupled problem in the fixed mesh $\widetilde{\mathscr{T}}_h^{n+1}$ by BFGS algorithm starting from the point $\boldsymbol{\alpha}^n$

$$\boldsymbol{\alpha}^{n+1}\in\arg\min_{\boldsymbol{\alpha}\in\mathbb{R}^m} J(\boldsymbol{\alpha})$$

where the cost function is computed as following:

(i) Solve the structure problem. We obtain $\mathbf{q}^{n+1}$ from (25), where $\boldsymbol{\alpha}^{n+1}$ was replaced by $\boldsymbol{\alpha}$. Then set the displacement of the structure $\mathbf{u}=\sum_{i=1}^m q_i^{n+1}\boldsymbol{\phi}^i$.
(ii) Solve the fluid problem (29)–(30) on the mesh $\widetilde{\mathscr{T}}_h^{n+1}$ under prescribed velocity at the fluid–structure interface (28) in order to get the fluid velocity $\mathbf{v}$ and pressure p.
(iii) Compute β_i from (36) for $i=1,\ldots,m$.
(iv) Set the cost function

$$J(\boldsymbol{\alpha})=\tfrac{1}{2}\|\boldsymbol{\alpha}-\boldsymbol{\beta}\|_{\mathbb{R}^m}^2$$

The gradient of the cost function is computed by finite differences.

Step 7: Update $\mathbf{q}^{n-1}\leftarrow\mathbf{q}^n$, $\mathbf{q}^n\leftarrow\mathbf{q}^{n+1}$, $\boldsymbol{\alpha}^{n-1}\leftarrow\boldsymbol{\alpha}^n$, $\boldsymbol{\alpha}^n\leftarrow\boldsymbol{\alpha}^{n+1}$, etc.

Remark 3
The major advantage of this implementation consists in using during *Step 6*, the same factorized matrix of the fluid problem obtained at *Step 5*. This was possible because the fluid mesh and the left side of Equations (29)–(30) do not depend on $\boldsymbol{\alpha}$. Only the right side of Equation (28) contains data ($\mathbf{q}^{n+1}$) that depends on $\boldsymbol{\alpha}$.

DOI: 10.1002/fld

5.2. The structure is governed by a non-linear model and solved by Newton's method

The stress at the interface $\mathbf{F}^{\mathrm{S},n+1}=(\sigma^{\mathrm{S}}\mathbf{n}^{\mathrm{S}})(t_{n+1})$ in the θ-scheme (26) is unknown. We approach the stress at the interface at the time instant t_{n+1} by $\sum_{i=1}^{m}\xi_i^{n+1}\boldsymbol{\psi}^i$ where ξ_i^{n+1} have to be identified and $\boldsymbol{\psi}^i\in(L^2(\Gamma_0))^2$ are shape functions. The shape functions $\boldsymbol{\psi}^i$ are not necessarily compatible with the structure or fluid finite element functions. Possible choices for $\boldsymbol{\psi}^i$ are polynomial functions [15], finite element like functions [34]. In this paper we have adopted $\boldsymbol{\psi}^i$ the solution of

$$a_{\mathrm{S}}(\boldsymbol{\psi}^i,\mathbf{w}^{\mathrm{S}})=\mu_i\int_{\Gamma_0}\boldsymbol{\psi}^i\cdot\mathbf{w}^{\mathrm{S}}\,\mathrm{d}\mathbf{X}\quad\forall\mathbf{w}^{\mathrm{S}}\in\mathbf{W}^{\mathrm{S}},\qquad\int_{\Gamma_0}\boldsymbol{\psi}^i\cdot\boldsymbol{\psi}^j\,\mathrm{d}\mathbf{X}=\delta_{ij}$$

Let us emphasize that, contrary to the eigenfunction $\boldsymbol{\phi}^i$, the traces of $\boldsymbol{\psi}^i$ are orthonormal for the scalar product of $L^2(\Gamma_0)$.

The implicit and semi-implicit time advancing algorithms when the structure is governed by a non-linear model are the same as for the linear model, excepting the definition of the cost function.

The *Step 1* in the implicit algorithm becomes: solve the optimization problem by BFGS method starting from the point $\boldsymbol{\xi}^n$,

$$\boldsymbol{\xi}^{n+1}\in\arg\min_{\boldsymbol{\xi}\in\mathbb{R}^m}J(\boldsymbol{\xi})$$

where the cost function is computed as following:

(i) Solve the structure problem (26) by Newton's method under the load $\mathbf{F}^{\mathrm{S},n+1}=\sum_{i=1}^{m}\xi_i\boldsymbol{\psi}^i$ and get the structure displacement $\mathbf{u}$. We recall that $a_{\mathrm{S}}(\cdot,\cdot)$ is non-linear in the first argument.
(ii) Build a fluid mesh $\mathscr{T}$ depending on the displacement $\mathbf{u}$.
(iii) Solve the fluid problem on the mesh $\mathscr{T}$ under prescribed velocity at the fluid–structure interface in order to get the fluid velocity $\mathbf{v}$ and pressure p.
(iv) Compute

$$\alpha_i=\int_{\Gamma_0}\left(\sum_{j=1}^{m}\xi_j\boldsymbol{\psi}^j\right)\cdot\boldsymbol{\psi}^i\,\mathrm{d}s,\quad\beta_i=-\int_{\Gamma_0}(\sigma^{\mathrm{F}}\mathbf{n}^{\mathrm{F}})_{(\mathbf{X}+\tilde{\mathbf{u}}(\mathbf{X},t),t)}\cdot\boldsymbol{\psi}^i\,\mathrm{d}s,\quad i=1,\ldots,m$$

(vi) Set the cost function

$$J(\boldsymbol{\alpha})=\tfrac{1}{2}\|\boldsymbol{\alpha}-\boldsymbol{\beta}\|^2_{\mathbb{R}^m}$$

Similarly, *Step 6* in the semi-implicit algorithm becomes: solve by BFGS the optimization problem

$$\boldsymbol{\xi}^{n+1}\in\arg\min_{\boldsymbol{\xi}\in\mathbb{R}^m}J(\boldsymbol{\xi})$$

where the cost function is computed as following:

(i) Solve the structure problem (26) by Newton's method under the load $\mathbf{F}^{\mathrm{S},n+1}=\sum_{i=1}^{m}\xi_i\boldsymbol{\psi}^i$ and get the structure displacement $\mathbf{u}$. We recall that $a_{\mathrm{S}}(\cdot,\cdot)$ is non-linear in the first argument.
(ii) Solve the fluid problem (29)–(30) on the mesh $\tilde{\mathscr{T}}_h^{n+1}$ under prescribed velocity at the fluid–structure interface $(\mathbf{u}-\mathbf{u}^n)/\Delta t$ in order to get the fluid velocity $\mathbf{v}$ and pressure p.
(iii) Compute

$$\alpha_i=\int_{\Gamma_0}\left(\sum_{j=1}^{m}\xi_j\boldsymbol{\psi}^j\right)\cdot\boldsymbol{\psi}^i\,\mathrm{d}s,\quad\beta_i=-\int_{\Gamma_0}(\sigma^{\mathrm{F}}\mathbf{n}^{\mathrm{F}})_{(\mathbf{X}+\tilde{\mathbf{u}}(\mathbf{X},t),t)}\cdot\boldsymbol{\psi}^i\,\mathrm{d}s,\quad i=1,\ldots,m$$

DOI: 10.1002/fld

(iv) Set the cost function

$$J(\boldsymbol{\alpha}) = \frac{1}{2}\|\boldsymbol{\alpha}-\boldsymbol{\beta}\|^2_{\mathbb{R}^m}$$

6. NUMERICAL RESULTS

The numerical tests have been produced using *FreeFem++* (see [35]).

The computation has been made in a domain of length $L=6\,\text{cm}$ and height $H=1\,\text{cm}$. The viscosity of the fluid was taken to be $\mu=0.035\,\text{g/cm}\cdot\text{s}$, its density $\rho^{\text{F}}=1\,\text{g/cm}^3$. The thickness of the elastic wall is $h^{\text{S}}=0.1\,\text{cm}$, the Young's modulus $E=3\times10^6\,\text{g/cm}\cdot\text{s}^2$, the Poisson ratio $\nu=0.3$, the density $\rho^{\text{S}}=1.1\,\text{g/cm}^3$. The Lamé parameters are computed by the formulas:

$$\lambda^{\text{S}}=\frac{\nu^{\text{S}}E}{(1-2\nu^{\text{S}})(1+\nu^{\text{S}})},\quad \mu^{\text{S}}=\frac{E}{2(1+\nu^{\text{S}})}$$

The volume force in fluid and structure are $\mathbf{f}^{\text{F}}=(0,0)^{\text{T}}$ and $\mathbf{f}^{\text{S}}=(0,0)^{\text{T}}$. The prescribed boundary stress at the inlet is

$$\mathbf{h}_{\text{in}}(\mathbf{x},t)=\begin{cases}(10^3(1-\cos(2\pi t/0.025)),0), & \mathbf{x}\in\Sigma_1,\ \ 0\leqslant t\leqslant 0.025\\ (0,0), & \mathbf{x}\in\Sigma_1,\ \ 0.025\leqslant t\leqslant T\end{cases}$$

and $\mathbf{h}_{\text{out}}=(0,0)$ at the outlet.

Remark 4

The above physical parameters correspond to the human blood flow in large arteries. Similar data were used in [2, 3] where the structure is governed by the generalized string model. The explicit algorithm based on the leap-frog scheme for the structure and on the backward Euler scheme for the fluid fails for this particular application (see [2]). Moreover, an implicit algorithm based on a classical fixed point iteration is unstable. A small relaxation parameter is necessary in order to get the stability of the fixed point iterations (see [3]). The same problem as in the present paper has been solved in [36], where the continuity of the velocity was treated by a Lagrange multiplier. The numerical results presented in [36] show that the continuity of the velocity is not very well respected and a small time step is necessary.

6.1. Linear elasticity. The structure is fixed at the left and at the right sides

We have used for the structure a reference mesh of 60 triangles and 62 vertices and for the fluid a reference mesh of 1250 triangles and 696 vertices. The meshes are not necessarily compatible at the interface (see Figure 3). The structure is fixed at the left and at the right sides.

For the approximation of the fluid velocity and pressure we have employed the triangular finite elements $\mathbb{P}_1+$*bubble* and $\mathbb{P}_1$, respectively. The finite element $\mathbb{P}_1$ was used in order to solve the eigenproblem of the structure.

The first eigenvalues are: $\lambda_{1,h}=7018.91$, $\lambda_{2,h}=50\,500$, $\lambda_{3,h}=193\,418$, $\lambda_{4,h}=529\,809$, $\lambda_{5,h}=832\,389$, $\lambda_{6,h}=1.13276\text{e}+06$, $\lambda_{7,h}=2.12627\text{e}+06$. For the physical parameters above and in view of the Remark 1, only the first $m=3$ modes have been considered for instant. More modes do not quantitatively change the value of the structure displacement.

The real parameter in the centered scheme (25) was chosen to be $\theta=0.25$.

DOI: 10.1002/fld

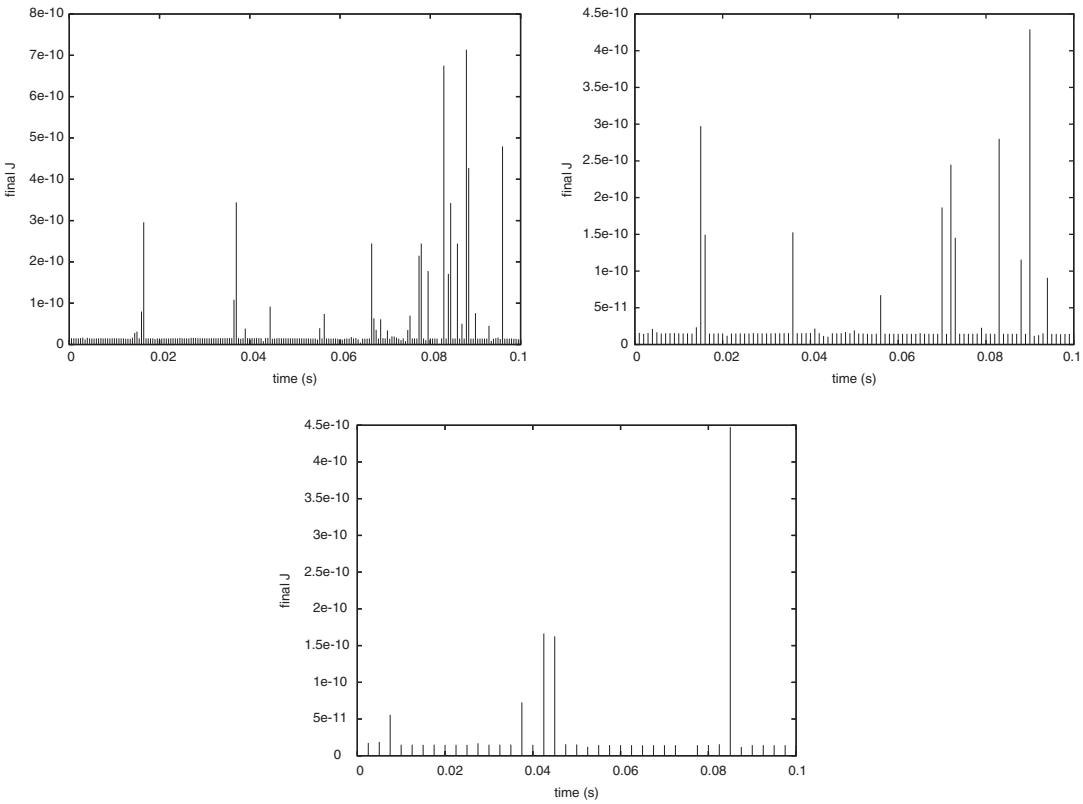

Figure 2. Linear elasticity. Time history of the final values of the cost function obtained by the BFGS method for $\Delta t = 0.0005$ (top, left), $\Delta t = 0.001$ (top, right), $\Delta t = 0.0025$ (bottom).

Stopping criteria and the mean number of cost function calls: We have performed the simulation for a time duration $T = 0.1$ s, with the time step $\Delta t = 0.001$ s and $N = 100$ time iterations.

At each time step, the optimization problem have been solved by the BFGS algorithm. The final values of the cost function are less than 4.5×10^{-10} (see Figure 2, top right). We have employed the *freefem++* implementation of the BFGS algorithm, which use the stopping criteria: $\|\nabla J\| < \varepsilon$ or the number of iterations reaches a maximal value *nbiter*.We have performed the computations with $\varepsilon = 10^{-4}$ and *nbiter* = 10. We set to 5 the maximal number of the iterations for the line search.

At each time step, the BFGS performs in average 6.08 iterations in the semi-implicit case and 6.24 iterations in the implicit case. At each BFGS iteration, 2.6 evaluations of the cost function are necessary in average for the line search and one call of the gradient. In this paper, we compute $\nabla J(\boldsymbol{\alpha})$ by the finite differences scheme

$$\frac{\partial J}{\partial \alpha_k}(\boldsymbol{\alpha}) \approx \frac{J(\boldsymbol{\alpha} + \Delta\alpha_k \mathbf{e_k}) - J(\boldsymbol{\alpha})}{\Delta\alpha_k}$$

where $\mathbf{e_k}$ is the kth vector of the canonical base of $\mathbb{R}^m$ and $\Delta\alpha_k = 10^{-6}$ is the grid spacing. Consequently, $m + 1 = 4$ calls of the cost function are needed in order to compute the gradient. To

DOI: 10.1002/fld

sum up, at each time step, the BFGS performs in average 40.24 evaluations of the cost function in the semi-implicit case and 41.61 iterations in the implicit case.

CPU time: The CPU time is 6 min and 14 s for $N=100$ time iterations and $\Delta t=0.001$ s on a computer with two processors of 3.6 GHz frequency.

In order to prove the superiority of the semi-implicit time advancing algorithm, we will compare with the CPU time obtained using implicit time advancing algorithm which is 71 min and 6 s. So the semi-implicit strategy is **11.34** times faster than the implicit one.

In the case of implicit strategy, at each evaluation of the cost function we have to solve one structure problem, to update the fluid mesh, to assembling the finite element matrix, to factorize it and to solve the fluid problem. We recall that, in the case of the semi-implicit time advancing algorithm, the evaluation of the cost function needs to solve a linear system, but what is of great practical importance consist in knowing a LU factorization of the matrix obtained at *Step 5*.

Computational gain on a finer fluid mesh: Also, we have performed the computations for a fluid mesh of 1632 vertices and 3052 triangles. In this case, the CPU time is 13 min and 53 s when the semi-implicit strategy is employed and 173 min and 52 s in the case of the implicit strategy, which gives that the first one is **12.52** faster than the second.

Computational reduction when the number of eigenfunctions is $m=7$: The CPU times is 193 min and 35 s in the case of the implicit strategy on fluid mesh of 1250 triangles and 696 vertices, when $m=7$. The semi-implicit scheme takes 14 min and 30 s, therefore we get a reduction of factor **13.31**.

Stability: We have performed the simulation for time steps: $\Delta t=0.0005, 0.001, 0.0025$ s. The final values of the cost function are less than 8×10^{-10} (see Figure 2). The semi-implicit algorithm has good stability properties, because the computed solution for moderate time steps are similar to the solution obtained by implicit method.

Behavior of the computed solution: The behavior of the fluid–structure interaction problem at different time instants is presented in Figures 3–6. A wave starts from the left side of the structure and it will be reflected at the right side. Movies with these simulations can be found at the address: http://www.edp.lmia.uha.fr/murea/.

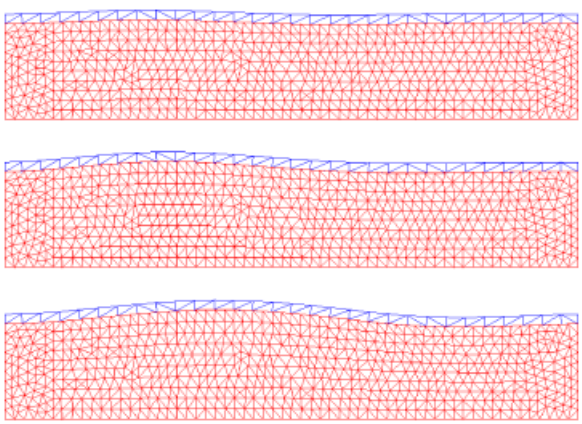

Figure 3. Linear elasticity. Fluid and structure meshes at time instant $t=0.015$ (top), $t=0.025$ (middle), and $t=0.035$ (bottom).

DOI: 10.1002/fld

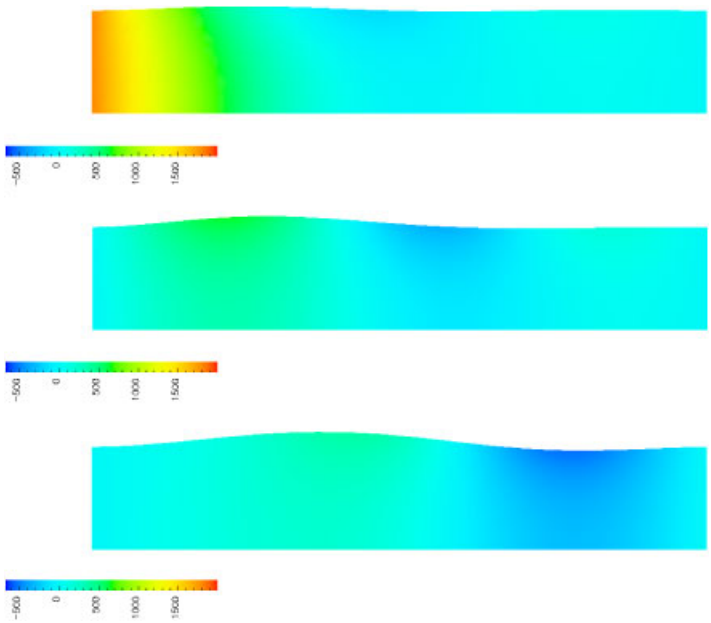

Figure 4. Linear elasticity. Fluid pressure [dynes/cm^2] at time instant $t=0.015$ (top), $t=0.025$ (middle), and $t=0.035$ (bottom).

6.2. *Linear elasticity. The structure is fixed at the left and free at the right*

In addition, we have performed simulation in the case when the horizontal displacement of the structure at the right side is supposed to be zero but the vertical displacement is free. In this case, when we build the discrete ALE map, the boundary condition on Σ_3 in problem (31)–(31) was replaced by

$$\widetilde{\mathbf{d}}^{n+1}(L,x_2)=\left(0,\frac{x_2\widetilde{u}_{h,2}(L,H)}{H}\right)\quad \forall x_2\in(0,H)$$

Fluid and structure meshes at different time instants are shown in Figure 7.

We have investigated the vertical displacement of three points on the interface of coordinates $x_1=L/4$, $x_1=L/2$, $x_1=3L/4$, respectively (see Figure 8). We recall that L denotes the length of the undeformed interface.

6.3. *Non-linear elasticity. The structure is fixed at the left and at the right sides*

We have used for the structure a reference mesh of 60 triangles and 62 vertices and for the fluid a reference mesh of 1250 triangles and 696 vertices. We use the same physical and numerical parameters as in the linear case. This time, at every cost function call, the structure problem is solved by the Newton's method. The finite element $\mathbb{P}_1$ was used in order to solve the linear system (27) at each Newton iteration.

DOI: 10.1002/fld

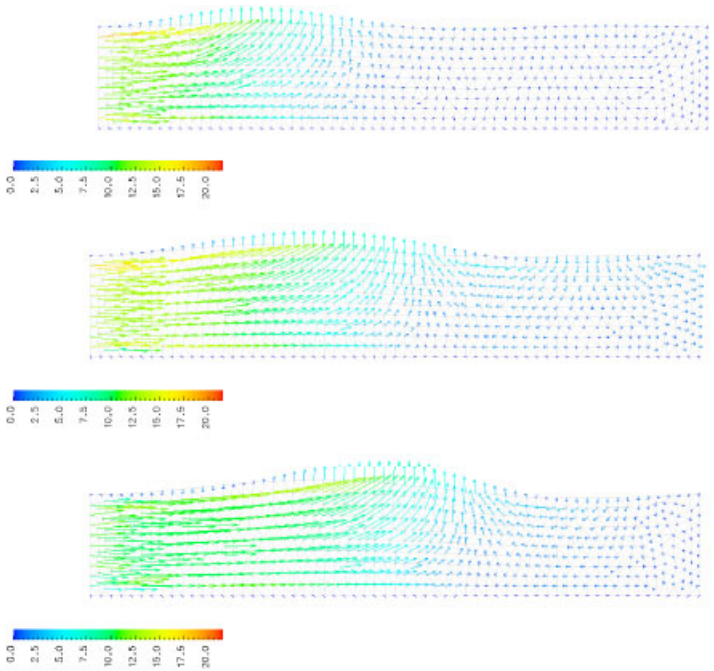

Figure 5. Linear elasticity. Fluid velocity [cm/s] at time instant $t=0.015$ (top), $t=0.025$ (middle), and $t=0.035$ (bottom).

The CPU time is 17 min and 13 s for $N=100$ time iterations and $\Delta t=0.001$ s on a computer with two processors of 3.6 GHz frequency. The CPU time obtained using implicit time advancing algorithm which is of 102 min and 26 s. So the semi-implicit strategy is **5.94** times faster than the implicit one.

At each time step, the BFGS performs in average 7.11 iterations in the semi-implicit case and 7.34 iterations in the implicit case. At each BFGS iteration, 2.62 evaluations of the cost function are necessary in average for the line search in the semi-implicit case and 2.60 iterations in the implicit case. One call of the gradient is necessary at each BFGS iteration for the both semi-implicit and implicit strategies. At each time step, the BFGS performs in average 47.10 evaluations of the cost function in the semi-implicit case and 48.48 iterations in the implicit case. Newton's method performs in average two iterations at every cost function call for the both semi-implicit and implicit strategies.

Figure 9 shows a good agreement between the solutions computed by the semi-implicit and implicit algorithm. In addition, we have performed simulation when the prescribed boundary stress at the inlet was magnified by a factor of 3. The maximal vertical displacement of the structure is about 0.6 cm. The fluid velocity is plotted in Figure 10.

6.4. Discussions

The CPU time ratio of implicit and semi-implicit algorithms is **11.34** when the structure is governed by linear elasticity model and solved by modal decomposition, while the same ratio is **5.94** when

DOI: 10.1002/fld

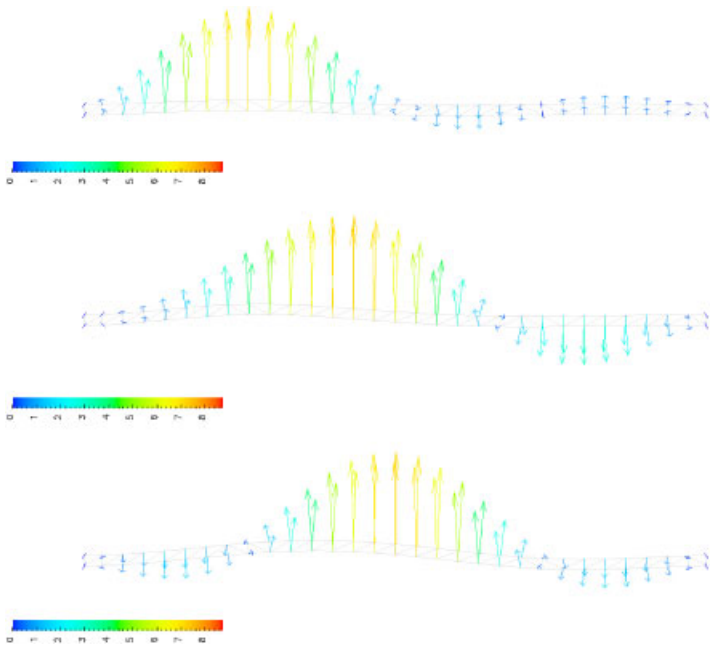

Figure 6. Linear elasticity. Structure velocity [cm/s] at time instant $t=0.015$ (top), $t=0.025$ (middle), and $t=0.035$ (bottom).

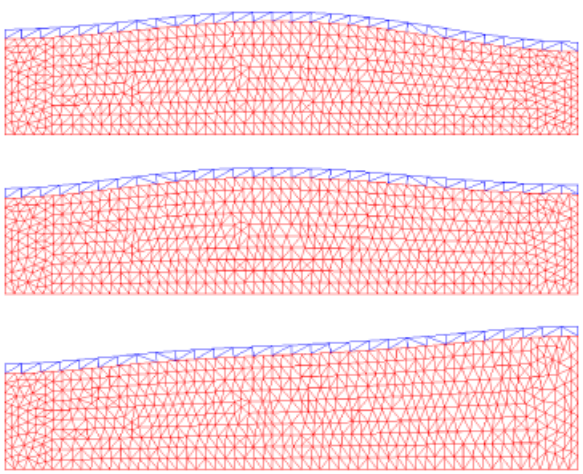

Figure 7. Linear elasticity and the left side of the structure is free. Fluid and structure meshes at time instant $t=0.050$ (top), $t=0.075$ (middle), and $t=0.100$ (bottom).

DOI: 10.1002/fld

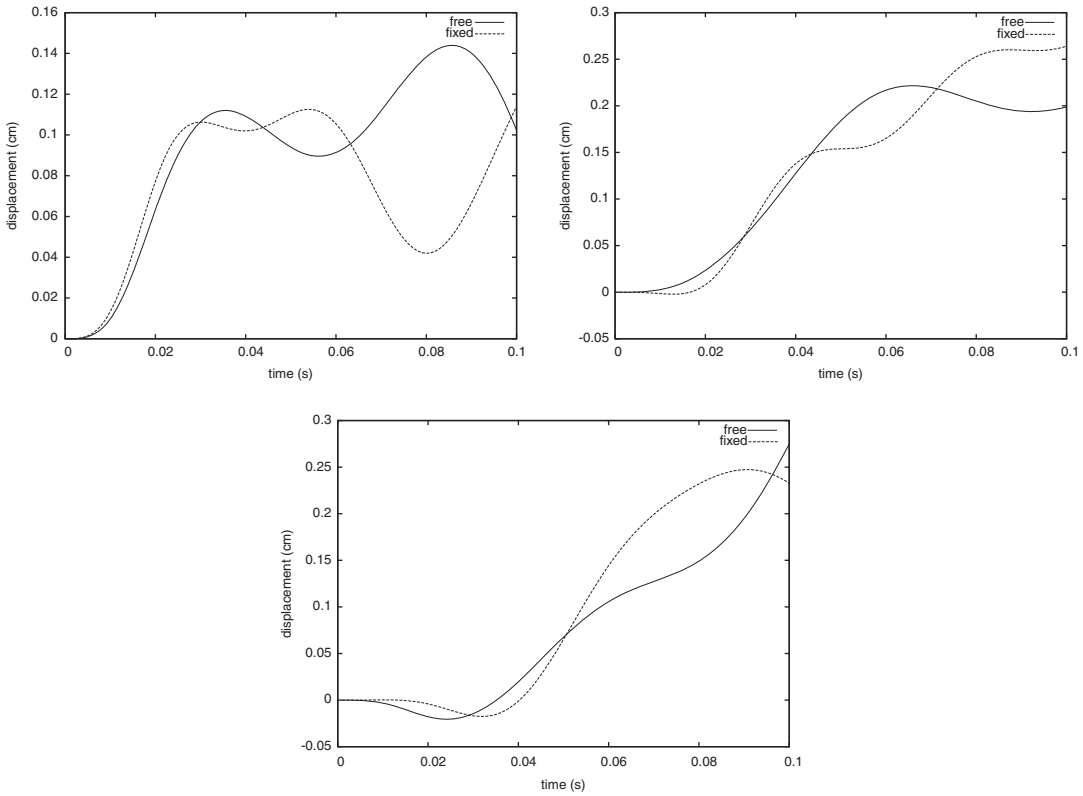

Figure 8. Linear elasticity. Time history of the vertical displacement of three points on the interface when the left side of the structure is fixed or free. Points of horizontal coordinate $x_1 = L/4$ (top, left), $x_1 = L/2$ (top, right), $x_1 = 3L/4$ (bottom).

the structure is non-linear and solved by Newton's method. In average, we have

$$\text{Total CPU time ratio} = \frac{N \times \text{CPU time for one time step (implicit)}}{N \times \text{CPU time for one time step (semi-implicit)}}$$

$$= \frac{\text{number of } J \text{ calls (implicit)}}{\text{number of } J \text{ calls (semi-implicit)}} \times \frac{\text{CPU time for one call of } J \text{ (implicit)}}{\text{CPU time for one call of } J \text{ (semi-implicit)}}$$

In the linear case, we have

$$11.34 = \frac{41.61}{40.24} \times \frac{\text{CPU time for one call of } J \text{ (implicit)}}{\text{CPU time for one call of } J \text{ (semi-implicit)}}$$

$$= \frac{41.61}{40.24} \times \frac{\text{CPU time fluid (implicit)} + \text{CPU time structure} + \text{CPU time other}}{\text{CPU time fluid (semi-implicit)} + \text{CPU time structure} + \text{CPU time other}}$$

DOI: 10.1002/fld

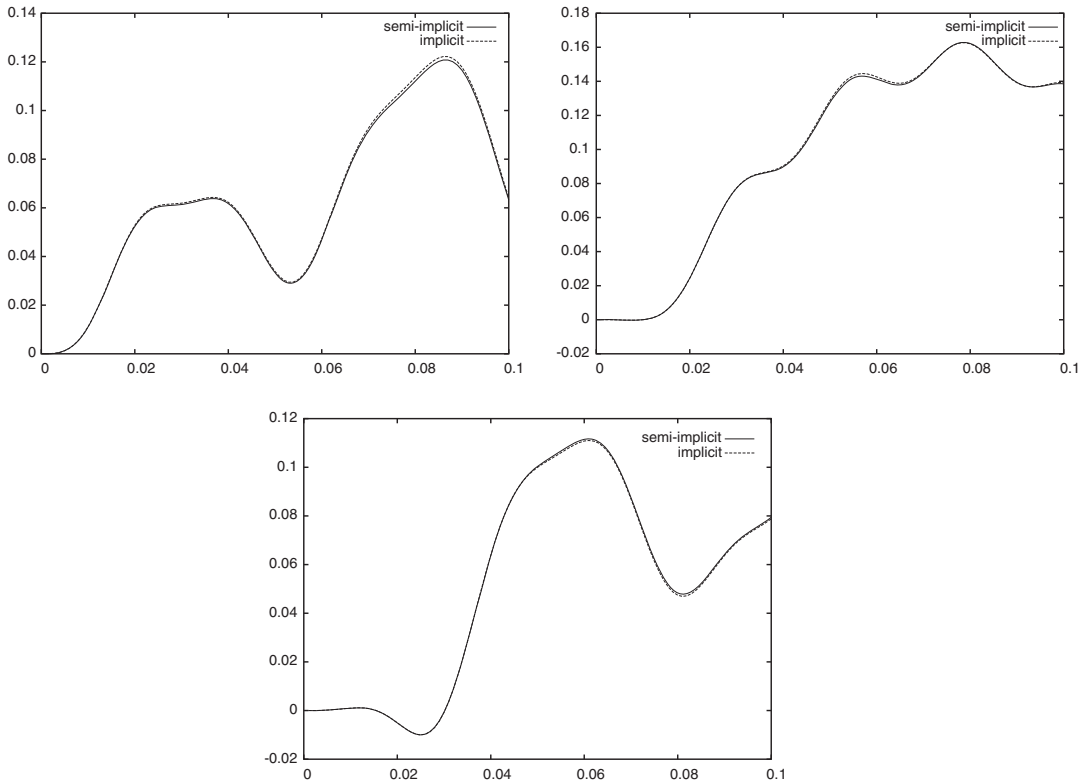

Figure 9. Non-linear elasticity. Time history of the vertical displacement of three points on the interface when the left side of the structure is fixed. Points of horizontal coordinate $x_1 = L/4$ (top, left), $x_1 = L/2$ (top, right), $x_1 = 3L/4$ (bottom). We observe a good agreement between the curves obtained by the implicit and semi-implicit algorithms.

and in the non-linear case, we have

$$5.94 = \frac{48.48}{47.10} \times \frac{\text{CPU time fluid (implicit)} + \text{CPU time structure} + \text{CPU time other}}{\text{CPU time fluid (semi-implicit)} + \text{CPU time structure} + \text{CPU time other}}$$

Since the CPU time fluid (implicit) is greater that the CPU time fluid (semi-implicit), the function

$$x \to \frac{\text{CPU time fluid (implicit)} + x + \text{CPU time other}}{\text{CPU time fluid (semi-implicit)} + x + \text{CPU time other}}$$

is decreasing for $x > 0$. This explains why in our application the ratio of the total CPU time decreases when the CPU time structure is longer, for example in the non-linear case.

The ratio of the total CPU time depends also on the ratio of the number of the cost function calls. In our application, we have employed the same BFGS method in order to solve the coupled fluid–structure problem at every time step. The ratio of the number of the cost function calls is $\frac{41.61}{40.24}$ for a linear structure and $\frac{48.48}{47.10}$ in the non-linear case. But, if we employ a better method for

DOI: 10.1002/fld

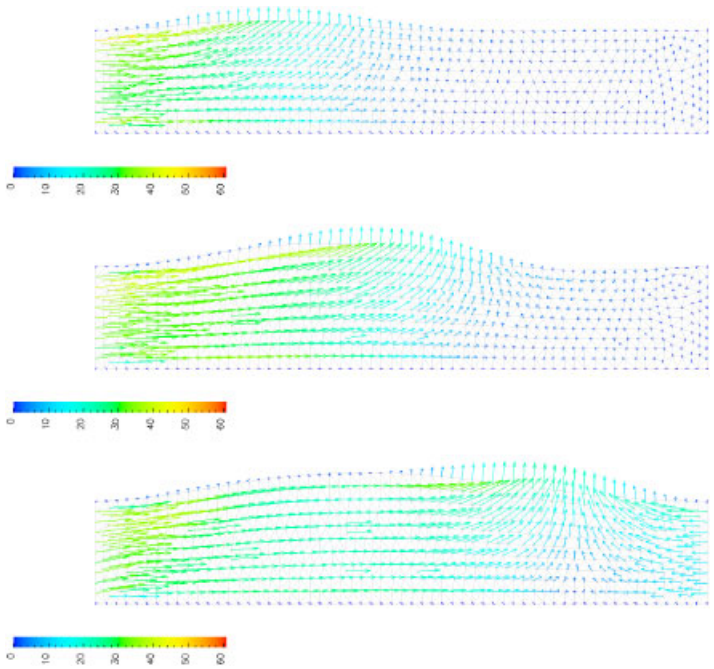

Figure 10. Non-linear elasticity. Fluid velocity [cm/s] at time instant $t=0.015$ (top), $t=0.025$ (middle), and $t=0.035$ (bottom).

solving the coupled fluid–structure problem in the semi-implicit algorithm, the denominators of the previous ratios decrease and then the ratio of the total CPU time increases.

A straightforward calculation leads to

$$\frac{\text{CPU time fluid (implicit)}}{\text{CPU time fluid (semi-implicit)}}$$

$$> \frac{\text{CPU time fluid (implicit)} + \text{CPU time structure} + \text{CPU time other}}{\text{CPU time fluid (semi-implicit)} + \text{CPU time structure} + \text{CPU time other}}$$

$$= 11.34 \times \frac{40.24}{41.61} = 11.06$$

which proves that the CPU time fluid is considerably reduced when the semi-implicit strategy is adopted to solve our particular application.

7. CONCLUSIONS

A semi-implicit algorithm for solving numerically an unsteady fluid–structure interaction problem was presented. At each time step, the position of the interface is predicted in a explicit way. The displacement of the structure, velocity and the pressure of the fluid are computed implicitly by solving at each time step an optimization problem such that the continuity of the velocity as well

DOI: 10.1002/fld

as the continuity of the stress hold at the interface. During the optimization process, the fluid mesh does not move, which reduces the computational effort. The semi-implicit algorithm has good stability properties even if the interface was computed explicitly.

REFERENCES

1. Farhat C, Lesoinne M. Two efficient staggered algorithms for the serial and parallel solution of three-dimensional nonlinear transient aeroelastic problems. *Computer Methods in Applied Mechanics and Engineering* 2000; **182**(3–4):499–515.
2. Nobile F. Numerical approximation of fluid–structure interaction problems with application to haemodynamics. *Ph.D. Thesis*, EPFL, Switzerland, 2001.
3. Causin P, Gerbeau JF, Nobile N. Added-mass effect in the design of partitioned algorithms for fluid–structure problems. *Computer Methods in Applied Mechanics and Engineering* 2005; **194**:4506–4527.
4. Forster C, Wall WA, Ramm E. Artificial added mass instabilities in sequential staggered coupling of nonlinear structures and incompressible viscous flows. *Computer Methods in Applied Mechanics and Engineering* 2007; **196**(7):1278–1293.
5. Le Tallec P, Mouro J. Fluid–structure interaction with large structural displacements. *Computer Methods in Applied Mechanics and Engineering* 2001; **190**(24–25):3039–3067.
6. Formaggia L, Gerbeau GF, Nobile F, Quarteroni A. On the coupling of 3D and 1D Navier–Stokes equations for flow problems in compliant vessels. *Computer Methods in Applied Mechanics and Engineering* 2001; **191**(6–7):561–582.
7. Fernandez MA, Le Tallec P. Linear fluid–structure stability analysis with transpiration. Part I: formulation and mathematical analysis. *Computer Methods in Applied Mechanics and Engineering* 2003; **192**:4805–4835.
8. Deparis S, Fernández MA, Formaggia L. Acceleration of a fixed point algorithm for fluid–structure interaction using transpiration conditions. *Mathematical Modelling and Numerical Analysis* 2003; **37**(4):601–616.
9. Steindorf J, Matthies HG. Partitioned but strongly coupled iteration schemes for nonlinear fluid–structure interaction. *Computers and Structures* 2002; **80**:1991–1999.
10. Gerbeau JF, Vidrascu M. A quasi-Newton algorithm on a reduced model for fluid–structure interaction problems in blood flows. *Mathematical Modelling and Numerical Analysis* 2003; **37**(4):631–648.
11. Fernandez MA, Moubachir M. A Newton method using exact Jacobians for solving fluid–structure coupling. *Computers and Structures* 2005; **83**(2–3):127–142.
12. Dettmer W, Perić D. A computational framework for fluid–structure interaction: finite element formulation and applications. *Computer Methods in Applied Mechanics and Engineering* 2006; **195**(41–43):5754–5779.
13. Tezduyar TE, Sathe S, Keedy R, Stein K. Space–time finite element techniques for computation of fluid–structure interactions. *Computer Methods in Applied Mechanics and Engineering* 2006; **195**:2002–2027.
14. Murea CM, Vazquez C. Sensitivity and approximation of coupled fluid–structure equations by virtual control method. *Applied Mathematics and Optimization* 2005; **52**(2):183–218.
15. Murea CM. The BFGS algorithm for a nonlinear least squares problem arising from blood flow in arteries. *Computer and Mathematics with Applications* 2005; **49**:171–186.
16. Murea CM. Numerical simulation of a pulsatile flow through a flexible channel. *ESAIM*: *Mathematical Modelling and Numerical Analysis* 2006; **40**(6):1101–1125.
17. Mbaye I, Murea CM. Numerical procedure with analytic derivative for unsteady fluid–structure interaction. *Communications in Numerical Methods in Engineering*, published online 13 July 2007; DOI: 10.1002/cnm.1031.
18. Fernandez MA, Gerbeau JF, Grandmont C. A projection semi-implicit scheme for the coupling of elastic structure with an incompressible fluid. *International Journal for Numerical Methods in Engineering* 2007; **69**(4):794–821.
19. Nobile F, Vergara C. An effective fluid–structure interaction formulation for vascular dynamics by generalized Robin conditions. *SIAM Journal on Scientific Computing* 2008; **30**(2):731–763.
20. Quarteroni A, Formaggia L. Mathematical modelling and numerical simulation of the cardiovascular system. In *Handbook of Numerical Analysis*, Ciarlet PG (ed.), vol. XII. North-Holland: Amsterdam, 2004; 3–127.
21. Chen H, Sheu T. Finite-element simulation of incompressible fluid flow in an elastic vessel. *International Journal for Numerical Methods in Fluids* 2003; **42**:131–146.
22. Baffico L. A characteristic-ALE formulation for a fluid–membrane interaction problem. *Communications in Numerical Methods in Engineering* 2005; **21**:723–734.
23. Swim EW, Seshaiyer P. A nonconforming finite element method for fluid–structure interaction problems. *Computer Methods in Applied Mechanics and Engineering* 2006; **195**:2088–2099.

24. Cai ZX, Luo XY. A fluid-beam model for flow in collapsible channel. *Journal of Fluids and Structures* 2003; **17**:125–146.
25. Heil M. An efficient solver for the fully coupled solution of large-displacement fluid–structure interaction problems. *Computer Methods in Applied Mechanics and Engineering* 2004; **193**(1–2):1–23.
26. Ciarlet PG. *Elasticité tridimensionnelle* (French). Research in Applied Mathematics, vol. 1. Masson: Paris, 1986.
27. Dautray R, Lions JL. *Analyse mathématique et calcul numérique pour les sciences et les techniques*, vol. 8. Masson: Paris, 1988.
28. Chambolle A, Desjardins B, Esteban M, Grandmont C. Existence of weak solutions for the unsteady interaction of a viscous fluid with an elastic plate. *Journal of Mathematical Fluid Mechanics* 2005; **7**(3):368–404.
29. Hughes Th. *The Finite Element Method*: *Linear Static and Dynamic Finite Element Analysis*. Dover: New York, 2000.
30. Temam R. *Navier–Stokes Equations*. North-Holland: Amsterdam, 1979.
31. Hron J, Turek S. A monolithic FEM/multigrid solver for an ALE formulation of fluid–structure interaction with applications in biomechanics. *Fluid–Structure Interaction*. Lecture Notes in Computer Science and Engineering, vol. 53. Springer: Berlin, 2006; 146–170.
32. Dennis Jr JE, Schnabel RB. *Numerical Methods for Unconstrained Optimization and Nonlinear Equations*. Classics in Applied Mathematics, vol. 16. Society for Industrial and Applied Mathematics: Philadelphia, PA, 1996.
33. Farhat C, Lesoinne M, Le Tallec P. Load and motion transfer algorithms for fluid/structure interaction problems with non-matching discrete interfaces: momentum and energy conservation, optimal discretization and application to aeroelasticity. *Computer Methods in Applied Mechanics and Engineering* 1998; **21**:95–114.
34. Mbaye I, Murea CM. Approximation par la méthode des moindres carrés d'un problm̀e bidimensionnel stationnaire d'interaction fluide-structure. *Proceedings of Euro-Mediterranean Conference on Bio-mathematics*, Cairo, 26–28 June 2007.
35. Hecht F, Pironneau O. A finite element software for PDE: FreeFem++. Available from: http://www.freefem.org (access on May 2008).
36. Murea CM. A semi-implicit algorithm based on the augmented Lagrangian method for fluid–structure interface. In *Numerical Mathematics and Advanced Applications*, Kunisch K, Of G, Steinbach O (eds), *Proceedings of ENUMATH 2007*, *The 7th European Conference on Numerical Mathematics and Advanced Applications*, Graz, Austria, September 2007. Springer: Heidelberg, 2008; 555–562.

DOI: 10.1002/fld